

In Vivo Contact Areas of Tibiotalar Joint Measured with Magnetic Resonance Imaging

Makoto SAKAMOTO¹, Yosei NODAGUCHI², Yuji TANABE³, Keisuke SASAGAWA³,
Yosuke KUBOTA⁴, Hidenori YOSHIDA¹ and Koichi KOBAYASHI¹

¹Department of Health Sciences, Niigata University School of Medicine, Niigata 951-8518, Japan

²Graduate School of Science & Technology, Niigata University, Niigata 950-2181, Japan

³Department of Mechanical Engineering, Niigata University, Niigata University, Niigata 950-2181, Japan

⁴Venture Business Laboratory, Niigata University, Niigata 950-2181, Japan

(Received 14 January 2010; received in revised form 21 May 2010; accepted 12 June 2010)

Abstract

In vivo contact areas of tibiotalar joints in 20 healthy subjects were studied using a loading device within a closed-MRI system. Cartilage-enhanced, sagittal images were obtained at 10° of dorsiflexion, and 0° and 10° of plantarflexion under 200 N ankle-loaded conditions. For ankle-unloaded conditions, the ankle was positioned at 10° of dorsiflexion, and 0°, 10°, 30°, and 50° of plantarflexion. This study highlights the differences in tibiotalar joint contact area between different ankle flexion postures, loading conditions, and geometries of joint surfaces.

Key words

Biomechanics, Tibiotalar Joint, Contact Area, Magnetic Resonance Imaging, Articular Cartilage

1. Introduction

The ankle joint complex connects the foot and leg, and consists of the tibiotalar, fibulotalar, and distal tibiofibular joints. It plays a fundamental role in human locomotion. The ankle joint mainly allows dorsiflexion and plantarflexion (Fig. 1). The compressive force on the ankle joint is approximately two to five times body weight during gait cycle [1-3].

Contact characteristics have been extensively studied in joints such as the knee and hip; however, there is relatively little information available for the ankle joint. Traditionally, such data have been obtained from *in vitro* cadaveric ankle specimens using dye-staining, casting techniques, pressure transducers, and pressure-sensitive films. In a pioneering study, Ramsey and Hamilton [4] used a dye-staining

technique to determine the contact area in 23 dissected tibiotalar articulations, with the talus in neutral position and displaced 1, 2, 4, and 6 mm laterally. Kimizuka et al. [5] used a silicon rubber casting technique and a pressure sensor to measure the contact area of 8 human cadaveric talocrural joints, and reported contact area of 522 mm² and maximum pressure of 9.9 MPa under 1500 N loading. Omori et al. [6] used a dynamic pressure rubber sensor to evaluate the effects of an ankle brace on the distribution of dynamic contact pressure in the tibiotalar joint with simulated lateral ligamentous injury. Pressure-sensitive films are the most widely used technique for measuring joint contact areas and pressure distributions in the tibiotalar joints [7-12]. For example, Harris and Fallat [11] utilized pressure-sensitive film to examine the tibiotalar contact area with lateral and posterosuperior displacement of the distal fibula while the deltoid ligament remains intact.

The use of cadaveric ankle specimens for contact area measurements is limited as the true physiological loading behavior of the muscles, tendons, and ligaments cannot be reproduced. Very few studies have reported *in vivo* joint contact characteristics of the tibiotalar joint. Recently, a technique using dual-orthogonal fluoroscopic images and magnetic resonance image-based computer models was described for the study of *in vivo* articular cartilage contact kinematics of the ankle [13-15]. The articular cartilage contact area was determined as the overlapping of the opposing cartilage layers, which represented a “theoretical” contact area. This treatment might result in an underestimation of the contact area because actual cartilage deformation would cause deformation beyond the edge of the overlapping area [14].

Magnetic resonance imaging (MRI) has recently been shown to be a valid method of quantifying patellofemoral joint contact area, indicating the potential for *in vivo* assessment [16-18]. In previous studies, the contact area was determined by directly measuring the length of visible contact between the patella and femur in each transverse or sagittal slice showing cartilage. Salsich et al. [16] used a closed-MRI system to estimate patellofemoral joint contact areas *in vivo* and compared quadriceps in the contracted and relaxed conditions. Besier et al. [17] estimated patellofemoral joint contact areas in a group of healthy, pain-free subjects in upright, weightbearing conditions. Sixteen subjects were scanned in an open configuration MRI scanner with a 580 mm vertical gap that enabled imaging in the upright, weightbearing posture. However,

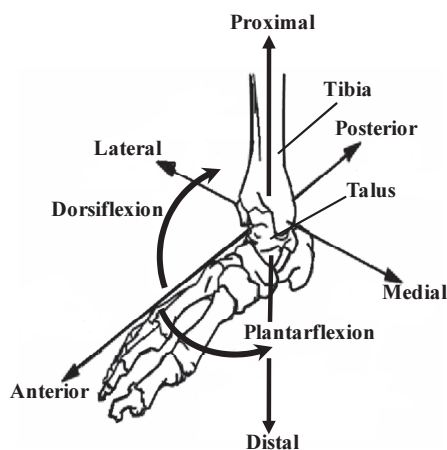


Fig. 1 Global coordinate system of the ankle joint

open configuration MRI systems are prone to partial volume artifacts. Sakamoto et al. [18] developed an *in vivo* closed-MRI system with a loading device that enables determination of the three-dimensional contact distributions of the patellofemoral joint during various degrees of knee flexion under knee-loaded conditions.

In the present paper, we adapted a closed-MRI system with a loading device [18] to study the *in vivo* articular cartilage contact areas and contact distributions of the tibiotalar joint during various ankle flexions under ankle-unloaded and ankle-loaded conditions. We also evaluated the effects of body height and the geometry of tibial and talar joint surfaces on the contact areas of the tibiotalar joints.

2. Materials and Methods

Twenty normal right ankles from 20 healthy subjects (age, 22-31 years; 14 male, 6 female) were examined. The average body height of the subjects was 170 ± 7.7 cm.

Resistance to an extensor mechanism was accomplished using a custom-built, non-ferromagnetic loading apparatus. This device enabled subjects to perform unilateral leg extension in the supine position (Fig. 2). Resistance to leg extension was accomplished by pushing against a footplate connected through a pulley system to a polyethylene water tank containing 200 N weights. Subjects were positioned with their right foot on the footplate, and the ankle was positioned at $+10^\circ$, 0° , and -10° of flexion (dorsiflexion: +, plantarflexion: -) under the ankle-loaded condition. The subjects maintained posture of the ankle within the flexion angles of 10° to -10° during image acquisition (approximately 7 min) with a load of 200 N. For the ankle-unloaded condition, the same subjects were positioned with their foot on the footplate, without any weight, and the ankle was positioned at 10° , 0° , -10° , -30° and -50° of flexion. After positioning of the ankle, the loading apparatus was moved into the MRI bore and imaging commenced.

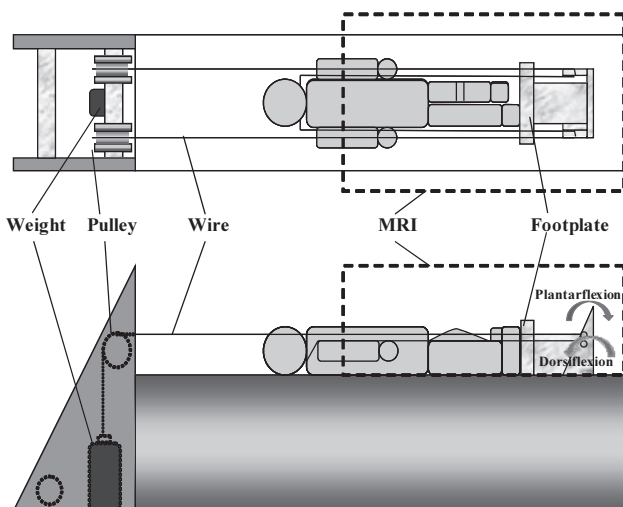


Fig. 2 Schematic of the subject and loading device in a closed-MRI system

Images were obtained at each angle of flexion in the loaded and unloaded conditions, using a 1.5 T closed-MRI system (Intera Achieva, Philips, Amsterdam, Netherlands). A 3D spectral presaturation with inversion recovery (SPIR) sequence was employed to obtain sagittal plane images of the tibiotalar joint in each posture. Using this pulse sequence, the cartilage appears bright (gray or white), and any separation between the cartilage surfaces is apparent as a dark line. Sagittal views were chosen to maximize the number of images across the tibiotalar joint contact area. Each scan took approximately 7 min, using the following parameters: TR (repetition time) = 40 ms, TE (echo time) = 10.2 ms, flip angle = 40° , field of view = 180 mm, matrix dimensions = 512×512 .

Sagittal plane images were displayed for analysis using medical imaging software (Osiris Windows Ver. 4.18, University of Geneva, Switzerland). The section of the image containing the tibiotalar joint was isolated and magnified (Fig. 3 (a)). Contact was defined as areas of tibia and talus approximation in which no distinct separation was visible between the cartilage borders of the joint surface. Because cartilage is relatively bright on images obtained with the SPIR sequence, the definition of contact area was operatively defined as ‘gray on gray.’ The line of contact between the tibia and talus was measured and recorded using the same software used to display the image. When the line of contact was curved, separate sort straight-line segments were measured (Fig. 3 (a)). To determine the contact area for each slice, the length of the line of contact was multiplied by the slice thickness of 1-mm (Fig. 3 (b)). Measurement of the contact area for each ankle flexion angle and each loading condition was performed three times in the same joint by a single observer and were found to be reproducible, with a coefficient of variation of approximately 3%. Three-dimensional contact distribution of the tibiotalar joint was determined using medical imaging software (Zed View,

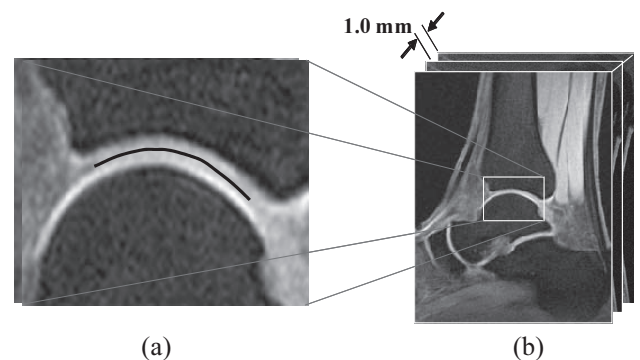


Fig. 3 (a) Representative sagittal plane image of the tibiotalar joint at magnification of approximately 3 times normal size. The black line indicates contact between the tibia and talus (b) Representative original image of the tibiotalar joint. Contact area was determined by measuring the length of contact between the tibia and talus in each slice, multiplying this length by slice thickness of 1-mm, and summing these values

LEXI, Tokyo, Japan) for three-dimensional modeling. This software generates and modifies three-dimensional surface models from stacked MR and computed tomography (CT) images via image segmentation. These analytical methods are highly reproducible, with results comparable with those of the established pressure-sensitive film technique [19].

To determine the effect of geometric congruity of the tibiotalar joint surface on contact area, we employed simple parameters at the sagittal middle portions of each bone (tibia and talus), defined as follows (Figs. 4 and 5):

$$\text{Curvature of tibial mortise (CTM)} = h_{ti} / l_{ti}, \quad (1)$$

$$\text{Curvature of talar dome (CTD)} = h_{ta} / l_{ta}, \quad (2)$$

where l_{ti} is the length of the tibial mortise, h_{ti} is the height of the tibial mortise, l_{ta} is the bottom length of the trochlea tali, and h_{ta} is the height of the trochlea tali.

3. Results and Discussion

Figure 6 shows the typical three-dimensional distribution of contact area of the cartilage layer on the talus in four subjects (#1 and #5 are male, and #18 and #19 are female) at different angles of flexion, under loaded (200 N) and unloaded (0 N) conditions. The contact area of the articular surface of the talus shifted from an anterior to a posterior region between dorsiflexion and plantarflexion under both load conditions. For flexion angles of 10° to -10°, the contact area at each flexion angle was slightly larger under the loaded condition than under the unloaded condition.

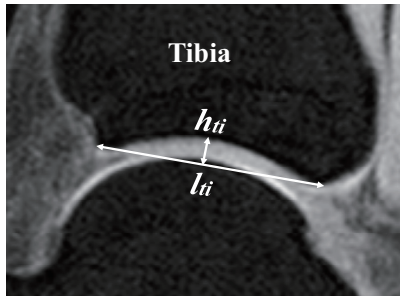


Fig. 4 Definition of curvature of the tibial mortise

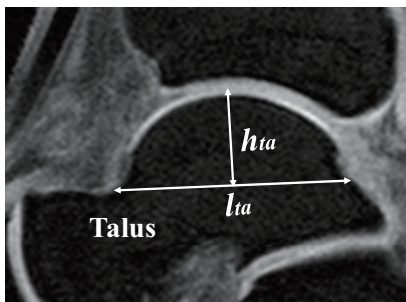


Fig. 5 Definition of curvature of the talar dome

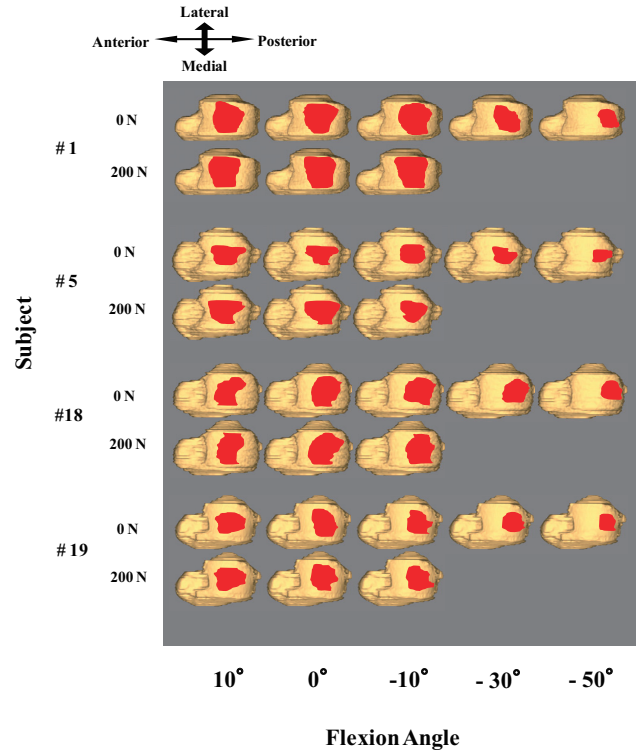


Fig. 6 Typical three-dimensional distributions of the contact area on the cartilage layer of the talus

Figure 7 shows the tibiotalar joint contact area at various ankle flexion angles under the unloaded and loaded conditions. For the unloaded condition, subjects displayed tibiotalar joint contact areas (average and standard deviation) of 298.2 ± 59.5 , 330.9 ± 66.7 , 283.0 ± 73.8 , 227.4 ± 66.1 , and 152.6 ± 41.5 mm² at 10°, 0°, -10°, -30°, and -50° of ankle flexion, respectively. For the loaded condition, contact areas were 321.2 ± 77.7 , 376.6 ± 72.7 , and 342.3 ± 71.0 mm² at 10°, 0°, and -10° of flexion, respectively; these values were significantly larger than those under the unloaded condition at flexion angles of 0° and -10° ($p < 0.01$). Increased ratios of contact areas in the

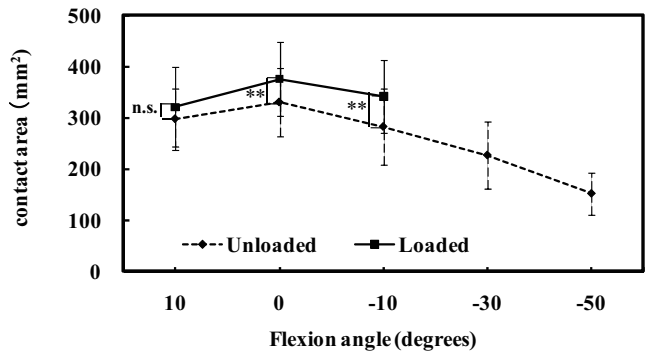


Fig. 7 Tibiotalar joint contact area at various ankle flexion angles under the unloaded and loaded conditions. Average and standard deviation are shown. Significant difference ($p < 0.01$) between unloaded and loaded conditions is indicated by **; n.s. indicates no significantly difference

200 N loaded conditions were approximately 14 and 21% for flexion angles of 0° and -10°, respectively.

Table 1 shows the available data from previous studies regarding contact area of the tibiotalar joint. Ramsey and Hamilton [4] measured an *in vitro* contact area of 440 ± 121 mm² in the neutral position under a compressive load of 700 N. Kimizuka et al. [5] reported an average *in vitro* contact area of 522 mm² in the neutral position under 1500 N compressive load. Macko et al. [7] measured *in vitro* contact areas of 540 ± 74, 522 ± 94, and 381 ± 93 mm² at 10° of dorsiflexion, neutral position (0°), and 15° of plantarflexion, respectively. The authors simulated these compressive loads of the ankle to approximate the maximum physiological loads experienced during walking. At 10° of dorsiflexion, neutral position, and 15° of plantarflexion, compressive loads were 3920, 2350, and 157 N, respectively. Driscoll et al. [8] also measured *in vitro* contact areas, and reported 284 ± 43, 327 ± 32, and 270 ± 41 mm² at 20° of dorsiflexion, neutral position, and 20° of plantarflexion, respectively. They applied an axial load of 800 N through the tibia, with 10% of the total load distributed through the fibula, to 18 cadaver specimens. Pereria et al. [10] reported average *in vitro* contact areas of 147, 167, and 149 mm² at 10° of dorsiflexion, neutral position, and 20° of plantarflexion, respectively, under a compressive load of 500 N. Wan et al. [13] investigated the *in vivo* contact areas of the tibiotalar joint of nine healthy ankles under weight-bearing conditions that simulated the stance phase of walking using a dual-orthogonal fluoroscopic imaging technique. They reported contact areas of 272.7 ± 61.1 mm² at heel strike (angle of dorsiflexion = 4.9 ± 8.1°) 416.8 ±

51.7 mm² at mid-stance, and 335.7 ± 64.5 mm² at toe-off (angle of plantarflexion = 0.2 ± 12.1°).

In the present study, the maximum average contact areas occurred at the neutral position: 376.6 ± 72.7 mm² and 330.9 ± 66.7 mm² under the loaded and unloaded conditions, respectively. The average contact areas at dorsiflexion and plantarflexion were less than those at the neutral position under both load conditions. Except for the result of Macko et al. [7], the relationship between the contact area and the angle of ankle flexion found in the present study was the same as that described in previous studies [8, 10, 13]. It is generally known that during plantarflexion, as occurs during the early stance phase of gait, the contact area is limited and the joint is incongruous. As the position of the joint progresses from neutral to dorsiflexion, as would occur during the mid-stance of gait, the contact area increases and the joint becomes more stable [20]. We also found that our *in vivo* results for contact areas under the unloaded condition were the same as the *in vitro* results reported by Driscoll et al. [8]. We consider that the results of the present study reflect the fact that the ankle joint was compressed by approximately 800 N by Achilles tendon, calcaneofibular ligament, anterior talofibular ligament, capsule, and peroneus longus in the unloaded *in vivo* ankle situation.

Figure 8 shows the normalized contact area at various flexion angles under the unloaded and loaded conditions. The normalized contact area was calculated by dividing the contact area by the joint surface of the talus. The normalized contact areas under the loaded condition were significantly larger than those under the unloaded condition at flexion angles of 0° and -10°. Wan et al. [13] estimated the normalized contact area under *in vivo* walking conditions, measuring 20.9 ± 3.6, 31.0 ± 5.0, and 25.8 ± 5.0% at heel strike, mid-stance, and toe-off positions, respectively. Our results of normalized contact areas under the loaded condition were 34.8 ± 6.6, 40.6 ± 5.3, and 37.9 ± 7.0% at flexion angles of 10°, 0°, and -10°, respectively. These values are slightly higher than those of Wan et al. [13].

Table 1 Tibiotalar joint contact area

(mm ²)				
Authors	Conditions & Methods	Dorsiflexion (deg.)	Neutral (0°)	Plantarflexion (deg.)
Ramsey & Hamilton [4]	<i>in vitro</i> Dye-staining	—	440 ± 121	—
Kimizuka et al. [5]	<i>in vitro</i> Casting	—	522	—
Macko et al. [7]	<i>in vitro</i> PSF*	540 ± 74 (10°)	522 ± 94	381 ± 93 (15°)
Driscoll et al. [8]	<i>in vitro</i> PSF*	284 ± 43 (20°)	327 ± 32	270 ± 41 (20°)
Hartford et al. [9]	<i>in vitro</i> PSF*	—	337 ± 52	—
Pereria et al. [10]	<i>in vitro</i> PSF*	147 (10°)	167	149 (20°)
Harris & Fallat [11]	<i>in vitro</i> PSF*	—	361.1	—
Wan et al. [13]	<i>in vivo</i> Fluoroscopy	272.7 ± 61.1 (4.9 ± 8.1°) Heel strike	416.8 ± 51.7 Mid-stance	335.7 ± 64.5 (0.2 ± 12.1°) Toe off
Present study	<i>in vivo</i> MRI Loaded	321.2 ± 77.7 (10°)	376.6 ± 72.7	342.3 ± 71.0 (10°)
	Unloaded	298.2 ± 59.5 (10°)	330.9 ± 66.7	283.0 ± 73.8 (10°) 227.4 ± 66.1 (30°) 152.6 ± 41.5 (50°)

PSF*: Pressure-Sensitive Film

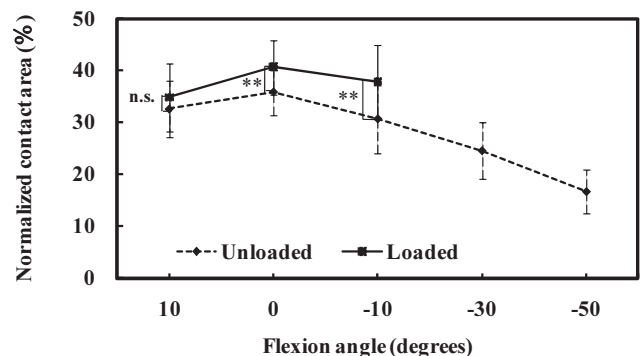


Fig. 8 Tibiotalar joint normalized contact area at various ankle flexion angles under the unloaded and loaded conditions. Average and standard deviation are shown. Significant difference ($p < 0.01$) between unloaded and loaded conditions is indicated by **; n.s. indicates no significant difference

In the present study, the parameters for curvature of the tibial mortise (CTM) did not differ significantly among the subjects (CTM = 0.128 ± 0.007); however, a negative linear correlation was found between curvature of the talar dome (CTD) and body height ($r = -0.60$), as shown in Fig. 9. Therefore, the simple parameter of CTD is a predictor of the geometry of the talar joint surface.

Figure 10 shows the relationship between the normalized contact area and CTD at the neutral position. The normalized contact area was negatively correlated with the CTD (loaded: $r = -0.66$; unloaded: $r = -0.60$). Our data suggest that when CTD is decreased, the talar dome is flattened and joint congruity is improved.

The present study has the following limitations. The first limitation is associated with our definition of joint contact. Our method was validated only by a previous study of the porcine knee joint [19]. In a future study, we will compare this method with others, such as application of pressure-sensitive film to a human cadaveric ankle joint.

The second limitation involves evaluation of supine positions of subjects. Our system applied load across the ankle, but may not capture all aspects of upright weight bearing.

The third limitation involves the magnitude of load. A 200 N load, which is lower than that encountered under physiological conditions, was chosen in view of the endurance of the subject during the MR imaging time. Average contact area in the present investigation was slightly less than that documented by Wan et al. [13];

however, the contact area and the normalized contact area were nearly identical. Thus, the findings of the current study regarding contact area and distribution are acceptably close to those in the physiological condition.

4. Conclusions

Use of a loading device within a closed-MRI system was shown to be a feasible tool for the direct measurement of *in vivo* contact areas of the tibiotalar joint at various angles of ankle flexion. Our results are summarized as follows.

(1) For the loaded condition with 200 N, average contact areas were 321.2 ± 77.7 , 376.6 ± 72.7 , and 342.3 ± 71.0 mm² at ankle positions of 10° (dorsiflexion), 0° (neutral position), and -10° (plantarflexion), respectively; these values are significantly larger than those under the unloaded condition and flexion angles of 0° and -10° ($p < 0.01$). The contact area on the articular surface of the talus shifted from anterior to posterior between dorsiflexion and plantarflexion.

(2) There was a negative linear correlation between curvature of the talar dome (CTD) and body height ($r = -0.60$).

(3) Normalized contact area at the neutral position was negatively correlated with CTD (loaded, $r = -0.66$; unloaded, $r = -0.60$).

Acknowledgements

This study was partially supported by a Grant-in-Aid for Scientific Research (c) 21560082 from the Japan Society for the Promotion of Science.

References

[1] Stauffer, R.N., Chao, E.Y.S. and Brewster, R.C.: Force and Motion Analysis of the Normal, Diseased, and Prosthetic Ankle Joint, *Clin. Orthop.*, **127**(1977), 189-196.
 [2] Procter, P and Paul, J.P.: Ankle Joint Biomechanics, *J. Biomech.*, **15**(1982), 627-634.
 [3] Nuber, G.W.: Biomechanics of the Foot and Ankle during Gait, *Clin. Sports Med.*, **7**(1988), 1-13.
 [4] Ramsey, P.L. and Hamilton, W.: Changes in Tibiotalar Area of Contact Caused by Lateral Talar Shift, *J. Bone Joint Surg. Am.*, **58**(1976), 356-357.
 [5] Kimizuka, M., Kurosawa, H. and Fukubayashi, T.: Load-bearing Pattern of the Ankle Joint. Contact Area and Pressure Distribution, *Arch. Orthop. Trauma Surg.*, **96**(1980), 45-49.
 [6] Omori, G., Kawakami, K., Sakamoto, M, Hara, T. and Koga, Y.: The effect of an Ankle Brace on the 3-dimensional Kinematics and Tibio-talar Contact Condition for Lateral Ankle Sprains, *Knee Surg. Traumatol. Arthrosc.*, **12**(2004), 457-462.
 [7] Macko, V.W., Matthews, L.S., Zwirkoski, P. and Goldstein, S.A.: The Joint-contact Area of the Ankle. The Contribution of the Posterior Malleolus, *J. Bone Joint Surg. Am.*, **73**(1991), 347-351.
 [8] Driscoll, H.L., Christensen, J.C. and Tencer, A.F.: Contact Characteristics of the Ankle Joint. Part 1. The normal joint, *J. Am. Podiatr. Med. Ass.*, **84**(1994), 491-498.

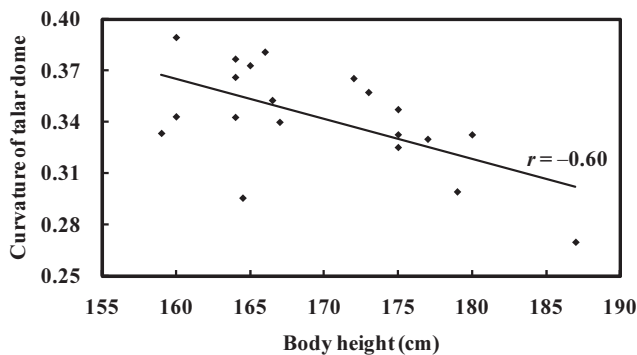


Fig. 9 Relationship between curvature of the talar dome (CTD) and body height

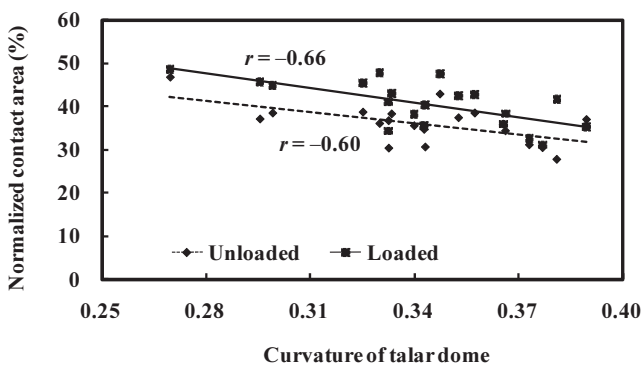


Fig. 10 Relationship between normalized contact area and curvature talar dome (CTD) at the neutral position

- [9] Hartford, J.M., Gorczyca, J.T., McNamara, J.L. and Mayor, M.B.: Tibiotalar Contact Area. Contribution of Posterior Malleolus and Deltoid Ligament, *Clin. Orthop. Relat. Res.*, **320**(1995), 182-187.
- [10] Pereira, D.S., Koval, K.J., Resnick, R.B., Sheskier, S.C., Kummer, F. and Zuckerman, J.D.: Tibiotalar Contact Area and Pressure Distribution: the Effect of Mortise Widening and Syndesmosis Fixation, *Foot Ankle Int.*, **17**(1996), 269-274.
- [11] Harris, J. and Fallat, L.: Effects of Isolated Weber B Fibular Fractures on the Tibiotalar Contact Area, *Foot Ankle Surg.*, **43**(2004), 3-9.
- [12] Anderson, D.D., Goldsworthy, J.K., Li, W., Rudert M.J., Tochigi, Y. and Brown, T.D.: Physical Validation of a Patient-Specific Contact Finite Element Model of the Ankle, *J. Biomech.*, **40**(2007), 1662-1229.
- [13] Wan, L., de Asla, R.J., Rubash, H.E. and Li, G.: Determination of In-vivo Articular Cartilage Contact Areas of Human Talocrural Joint under Weightbearing Conditions, *Osteoarthritis Cartilage*, **14**(2006), 1294-1301.
- [14] Li, G., Wan, L., and Kozanek, M.: Determination of Real-time In-vivo Cartilage Contact Deformation in the Ankle Joint, *J. Biomech.*, **41**(2008), 128-136.
- [15] de Asla, R.J., Kozánek, M., Wan, L., Rubash, H.E. and Li, G.: Function of Anterior Talofibular and Calcaneofibular Ligaments during In-vivo Motion of the Ankle Joint Complex, *J. Orthop. Surg. Res.*, **16**(2009), 4-7.
- [16] Salsich, G.B., Ward, S.R., Terk, M. and Poweres, C.M.: In Vivo Assessment of Patellofemoral Joint Contact Area in Individuals. Who are Pain Free, *Clin. Orthop. Rel. Res.*, **417**(2003), 277-284.
- [17] Besier, T.F., Draper, C.E., Gold, G.E., Beaupré, G.S. and Delp, S.L.: Patellofemoral Joint Contact Area Increases with Knee Flexion and Weight-bearing, *J. Orthop. Res.*, **23**(2005), 345-50.
- [18] Sakamoto, M., Shimoda, M., Kobayashi, K., Yoshida, H. and Tanabe, Y.: Analysis of Patellofemoral Joint Contact Area Using Magnetic Resonance Imaging (in Japanese), *Japanese J. Soc. Clin. Biomech.*, **28**(2007), 161-166.
- [19] Yoshida, H., Kobayashi, K., Sakamoto, M. and Tanabe, Y.: Determination of Joint Contact Area Using MRI (in Japanese), *Japanese J. Radiological Technology*, **65**(2009), 1025-1032.
- [20] Kaufman, K.R. and An, K.N.: Joint-Articulating Surface Motion, *The Biomedical Engineering Handbook* (Bronzino, J.D. eds.), CRC Press (2000), 20-1-20-37.